CrossMark
click for updates

Activation of an Otherwise Silent Xylose Metabolic Pathway in *Shewanella oneidensis*

Ramanan Sekar, Hyun Dong Shin, Thomas J. DiChristina

School of Biology, Georgia Institute of Technology, Atlanta, Georgia, USA

ABSTRACT

Shewanella oneidensis **is unable to metabolize the sugar xylose as a carbon and energy source. In the present study, an otherwise silent xylose catabolic pathway was activated in** *S. oneidensis* **by following an adaptive evolution strategy. Genome-wide scans indicated that the** *S. oneidensis* **genome encoded two proteins similar to the xylose oxido-reductase pathway enzymes xylose reductase (SO_0900) and xylulokinase (SO_4230), and purified SO_0900 and SO_4230 displayed xylose reductase and xylulokinase activities, respectively. The** *S. oneidensis* **genome was missing, however, an** *Escherichia coli* **XylE-like xylose transporter. After 12 monthly transfers in minimal growth medium containing successively higher xylose concentrations, an** *S. oneidensis* **mutant (termed strain XM1) was isolated for the acquired ability to grow aerobically on xylose as a carbon and energy source. Whole-genome sequencing indicated that strain XM1 contained a mutation in an unknown membrane protein (SO_1396) resulting in a glutamine-to-histidine conversion at amino acid position 207. Homology modeling demonstrated that the Q207H mutation in SO_1396 was located at the homologous xylose docking site in XylE. The expansion of the** *S. oneidensis* **metabolic repertoire to xylose expands the electron donors whose oxidation may be coupled to the myriad of terminal electron-accepting processes catalyzed by** *S. oneidensis.* **Since xylose is a lignocellulose degradation product, this study expands the potential substrates to include lignocellulosic biomass.**

IMPORTANCE

The activation of an otherwise silent xylose metabolic system in *Shewanella oneidensis* **is a powerful example of how accidental mutations allow microorganisms to adaptively evolve. The expansion of the** *S. oneidensis* **metabolic repertoire to xylose expands the electron donors whose oxidation may be coupled to the myriad of terminal electron-accepting processes catalyzed by** *S. oneidensis.* **Since xylose is a lignocellulose degradation product, this study expands the potential substrates to include lignocellulosic biomass.**

Xylose is one of the primary products of lignocellulose degradation and, after glucose, is the second most abundant carbohydrate in nature. The xylose polymer xylan is the primary constituent of hemicellulose, which comprises approximately 17% of the dry weight of hardwoods and up to 31% of plants (1). Xylose catabolism is a key component of sustainable processes that produce useful secondary products from lignocellulosic biomass (2–4). Xylose catabolism is also of commercial interest because xylose conversion to useful secondary chemicals such as bioethanol and biodegradable plastics can reduce losses associated with lignocellulose bioprocessing (5, 6). Industrially important by-products of xylose metabolism include xylitol, which is used as a natural sweetener in the food and confectionary industries (7).

Xylose metabolic pathways include the oxido-reductase, isomerase, and Weimberg-Dahms pathways (Fig. 1) (1, 8). Extracellular xylose is transported inside the cell via the ATP-binding cassette (ABC) and major facilitator superfamily (MFS) xylose transporters XylFGH and XylE, respectively (9, 10). In the oxidoreductase pathway of *Pichia stipitis* (11), NAD(P)H-dependent D-xylose (referred to below as xylose) reductase converts intracellular xylose to xylitol, which is then oxidized to xylulose by D-xylitol dehydrogenase. Xylulose is then phosphorylated by xylulokinase to xylulose 5-phosphate, which enters the pentose phosphate pathway. In the xylose isomerase pathway of *Escherichia coli* (11), xylose isomerase converts xylose to xylulose, which enters the pentose phosphate pathway, similar

to the oxidoreductase pathway (1, 12). In the Weimberg-Dahms pathway of *Caulobacter crescentus*, xylose dehydrogenase catalyzes the conversion of xylose to xylonolactone, which is then converted either to α-ketoglutaric semialdehyde via the Weimberg pathway or to glucoaldehyde and pyruvate via the Dahms pathway (8).

The metal-reducing facultative anaerobe *Shewanella oneidensis* displays a variety of diverse metabolic systems that couple the oxidation of a wide variety of electron donors (13) to the reduction of a set of electron acceptors whose redox potentials span nearly the entire continuum of potentials encountered in nature (14). Recently, the list of electron donors has been expanded to include glucose and glycerol through adaptive evolution and metabolic engineering (15–17). Genes encoding canonical xylose
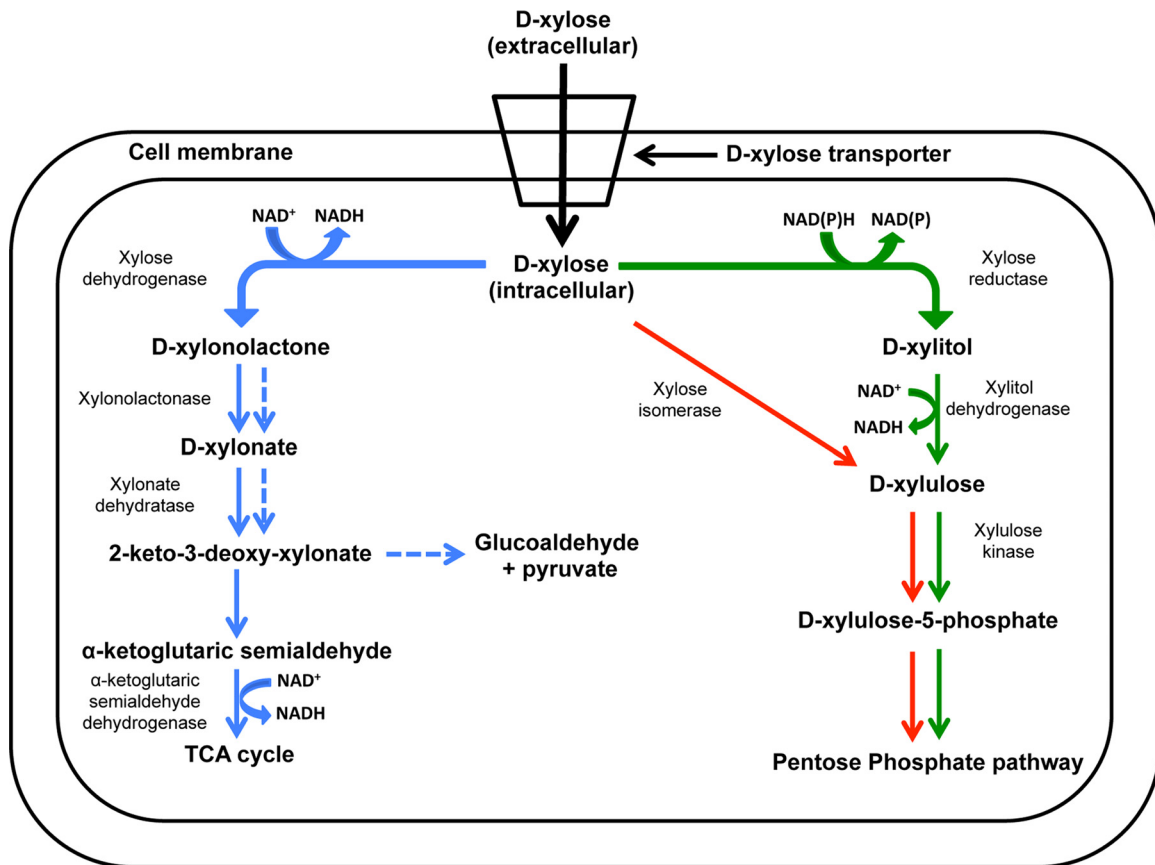
FIG 1 Xylose metabolic pathways in microorganisms. Solid blue, Weimberg pathway; dashed blue, Dahms pathway; solid red, isomerase pathway; solid green, oxidoreductase pathway.

metabolic pathways, however, are missing from the *S. oneidensis* genome (18).

In the present study, an adaptive evolution approach was followed to generate *S. oneidensis* mutants that metabolize xylose as the sole carbon and energy source. In adaptive evolution, mutations occur accidentally and a subset of the cell population acquires a mutation that facilitates growth under a new set of environmental conditions (19). Mutator cells include "growth advantage in stationary phase" (GASP) mutants in which genetic alterations in small cell populations display a higher competitive advantage over weaker cells (20). Adaptive evolution is a useful strategy for strain improvement in metabolic engineering (21–23) since *a priori* knowledge of the targeted metabolic process is not required (6). The remarkable metabolic flexibility displayed by *S. oneidensis* (24) led us to hypothesize that under selective growth conditions *S. oneidensis* mutator cells may acquire xylose metabolic capability.

The main objectives of the present study were to (i) adaptively evolve *S. oneidensis* to metabolize xylose as a carbon and energy source, (ii) identify the genes mutated in the adaptively evolved xylose catabolic pathway of *S. oneidensis*, (iii) identify and clone genes putatively encoding the xylose catabolic pathway, (iv) purify the corresponding proteins and determine their specific enzyme activities, and (v) determine the ability of the xylose-adapted strain to grow aerobically and anaerobically with xylose as the sole electron donor.

MATERIALS AND METHODS

Bacterial strains and growth conditions. Bacterial strains and plasmids used in this study are listed in Table 1. *S. oneidensis* and *E. coli* were routinely cultured aerobically on LB medium (10 g/liter of tryptone, 5 g/liter of yeast extract, and 10 g/liter of NaCl) at 30°C and 37°C, respectively (25). When required for selection, chloramphenicol (25 μg ml⁻¹), ampicillin (100 μg ml⁻¹), and gentamicin (15 μg ml⁻¹) were added to basal growth medium. Fe(III) citrate was prepared by previously described procedures (26, 27) and added at a final concentration of 10 mM. All chemical reagents were obtained from Sigma-Aldrich.

Adaptive evolution of *S. oneidensis* to metabolize xylose as the sole carbon and energy source. Wild-type (WT) *S. oneidensis* cells were initially grown in SM minimal medium for 48 h with 18 mM lactate as the sole carbon and energy source (see Table S1 in the supplemental material) (28). The cell culture was subsequently serially transferred each month over a 12-month period to fresh SM medium with increasing ratios of xylose to lactate (Table 2). The final mutant mix was plated on LB agar, and single colonies were screened for xylose utilization via the dinitrosalicylic acid (DNS) assay (29), which facilitates visual detection of reducing sugars. After 12 months, xylose-adapted *S. oneidensis* strain XM1 was isolated and grew aerobically with 65 mM xylose as the sole carbon and energy source. To facilitate identification of the xylose metabolic pathway in *S. oneidensis* strain XM1, the genome was sequenced with 300× coverage on an Illumina sequencing platform, assembled and analyzed with the CLC Workbench software (CLC BioQiagen, Aarhus, Denmark) together with the NCBI database (30) and modeling software I-TASSER (31).

Overall respiratory activity of xylose-adapted *S. oneidensis* XM1. The *S. oneidensis* wild type and the xylose-adapted mutant strain XM1

TABLE 1 Strains and plasmids used in this study

Strain or plasmid	Feature(s)	Source or reference
Shewanella oneidensis strains		
MR-1 (ATCC 700550)	Wild-type strain	ATCC
XM1	Xylose-adapted strain	This study
XM1-ΔSO1396^{Q207H}	Xylose-adapted strain with SO_1396^{Q207H} gene deleted	This study
XM1-ΔSO1396^{Q207H} + pBBR1MCS-SO_1396^{Q207H}	Xylose-adapted strain with SO_1396^{Q207H} deleted harboring pBBR1MCS with SO_1396^{Q207H} complementation	This study
XM1-ΔSO0900	Xylose-adapted strain with SO_0900 gene deleted	This study
XM1-ΔSO4230	Xylose-adapted strain with SO_4230 gene deleted	This study
EC100D pir-116	F$^-$ *mcrA* Δ(*mrr-hsdRMS-mcrBC*) φ80d*lacZ*ΔM15 Δ*lacX74 recA1 endA1 araD139* Δ(*ara leu*)7697 *galU galK* λ$^-$	Epicentre
Escherichia coli strains		
β2155 λ *pir*	*thrB1004 pro thi strA hsdS lacZM15* (F *lacZ*ΔM15 *lacI*^{q} *traD36 proA1 proB1*) Δ*dapA*::*erm pir*::RP4 Km^r	51
JM109 (ATCC 69905)	*endA1 gln V44 thi-1 relA1 gyrA96 recA1 mcrB$^+$* Δ(*lac-proAB*) e14$^-$ [F′ *traD36 proAB$^+$ lacI^q lacZ*ΔM15] *hsdR17*(r$_K$$^-$ m$_K$$^+$)	ATCC
JM109 pQE80L-0900	JM109 complemented with pQE80L harboring SO_0900 gene	This study
JM109 pQE80L-4673	JM109 complemented with pQE80L harboring SO_4673 gene	This study
JM109 pQE80L-4230	JM109 complemented with pQE80L harboring SO_4230 gene	This study
JM109 pQE80L-2452	JM109 complemented with pQE80L harboring SO_2452 gene	This study
Plasmids		
pKO2.0	4.5-kb γR6K, *mob* RP4 *sacB* Gm^r *lacZ* T5 promoter	This study
pBBR1MCS	4.7 kb; Cm^r *lacZ*	52
pBBR1MCS-SO_1396^{Q207H}	Plasmid with SO_1396^{Q207H} inserted	This study
pQE80L	4.8 kb; ColE1 Amp^r *lacI*^{q} 6× His (N terminal)	Qiagen
pQE80L-SO_0900	Plasmid with the SO_0900 gene inserted	This study
pQE80L-SO_4230	Plasmid with the SO_4230 gene inserted	This study
pQE80L-SO_2452	Plasmid with the SO_2452 gene inserted	This study

were tested for aerobic and anaerobic growth with 5 mM xylose, glucose, arabinose, galactose, lactose, sucrose, cellobiose, fructose, maltose, mannose, mannitol, trehalose, xylitol, or gluconate as the electron donor and either O_2, 5 mM nitrate ($NO_3$$^-$), 10 mM fumarate, or 10 mM Fe(III) citrate as the terminal electron acceptor. The cell cultures were incubated at 30°C for 68 h, and samples were withdrawn periodically for determination of cell density (optical density at 600 nm [OD_{600}]), nitrite, and Fe(II) concentrations.

Cloning and expression of *S. oneidensis* xylose-metabolizing genes in *E. coli.* The primers used for cloning genes SO_0900, SO_4673, SO_4230, and SO_2452 are listed in Table 3. These primers were used to PCR amplify the full-length genes from the *S. oneidensis* genome. The amplified genes were ligated into plasmid pQE80L (containing a His tag at

TABLE 2 Xylose and lactate concentrations during adaptive evolution of *S. oneidensis* over a 12-month period in fresh SM medium

Mo	Concn (mM) of:	
	Lactate	Xylose
1	18	0
2	18	5
3	15	10
4	12	15
5	10	20
6	10	30
7	7	35
8	5	40
9	5	50
10	3	55
11	1	65
12	0	65

the N terminus to facilitate protein purification) and transformed into *E. coli* JM109. The resulting recombinant strains were cultured in LB medium with 100 μg ml^{-1} of ampicillin at 37°C and induced with 1 mM isopropyl-β-D-thiogalactopyranoside (IPTG) at 25°C for 24 h for expression of SO_0900, SO_4673, SO_4230, and SO_2452.

Preparation of cell-free extract and protein purification. *E. coli* cells were prepared according to previously described procedures (32). Following protein expression in the presence of 1 mM IPTG, *E. coli* recombinant strains were harvested by centrifugation at 5,000 × *g* at 4°C for 30 min. Cells were washed once with extraction buffer (10 mM Tris-HCl at pH 7.5). Washed cell pellets were stored at −20°C until use. Cell pellets were resuspended to an OD_{600} of 50 in the equilibration buffer (50 mM Na_2HPO_4, 300 mM NaCl, and 10 mM imidazole at pH 8) and sonicated (8 cycles of 10 s with a 30-s cooling period). Cell debris was discarded after centrifugation at 16,000 × *g* for 20 min at 4°C. Supernatant was used as the cell extract, and the Bradford assay was used for estimation of protein concentration in the extract.

His-tagged protein in the cell extract was purified at 4°C using a HIS-Select HF nickel affinity gel (Sigma-Aldrich), which employs immobilized metal-ion affinity chromatography (IMAC) according to the manufacturer's small-scale purification protocol. Six-hundred-microliter aliquots of the cell extract were added to 150 μl of affinity gel in equilibration buffer. After overnight incubation, the gel was washed five times with equilibration buffer. The bound His-tagged protein was then eluted using 100 μl of elution buffer (50 mM Na_2HPO_4, 300 mM NaCl, and 250 mM imidazole at pH 8). Imidazole was removed by overnight dialysis at 4°C using extraction buffer as the dialysis solution. The purified protein product was used for SDS-PAGE analysis, determination of protein concentration, and activity assays.

Activity assays for protein expression. Xylose reductase activity was determined in McIlvaine buffer at pH 7.2 (prepared by adding 16.5 ml of 0.2 M Na_2HPO_4 to 3.5 ml of 0.1 M citric acid) containing 0.35 mM NADPH and 200 mM xylose and purified protein SO_0900 (32). For

TABLE 3 Primers used in this study[a]

Gene/operon	Primer	Sequence (5′ to 3′)
SO_1396[Q207H] (knockout)	SO_1396TF	CTCGATACCAGCCCATTTACG
	SO_1396D1BamHI	GACT<u>GGATCC</u>GCAATGGACCCTCGGCGATATGC
	SO_1396D2	CGTCATTATTTGGTATCAATCGTGGACGGCTAAGCCTCGAATCGC
	SO_1396D3	GCGATTCGAGGCTTAGCCGTCCACGAGATTGATACCAAATAATGACG
	SO_1396D4SalI	GACT<u>GTCGAC</u>GGTGATTGATGGCTCGAACAGCTTGG
	SO_1396TR	GCTGCAAACCAACTTTTCATGG
	SO_1396fwdseq	GAAGATATTGGCGAATAACCAACC
	SO_1396revseq	GTGGTCGATTCTTTTGAGAACG
	SO_1396fwdinsideseq	GCCGAGCAATACAGTGCTTGG
	SO_1396revinsideseq	CTCAGCATGACAATAATGTCTG
SO_0900 (knockout)	SO_0900TF	GCAGCGCAGTCCACAGGCCACTATTAA
	SO_0900D1BamHI	GACT<u>GGATCC</u>CGTCTAAGCCATTGCAGCGGATCAC
	SO_0900D2	CTAAGGACAGGGCAATCTAAATTGGCGGTATGCGTCTGTATTCCAT
	SO_0900D3	ATGGAATACAGACGCATACCGCCAATTTAGATTGCCCTGTCCTTAG
	SO_0900D4SalI	GACT<u>GTCGAC</u>GCTTGCATCACTTGCAACGACTGCGC
	SO_0900TR	GCTTCAAGCAGGGGATAATCGTCG
SO_4230 (knockout)	SO_4230TF	CCACATAGGGCTCACTGG
	SO_4230D1BamHI	GACT<u>GGATCC</u>GGTCTATATGGGTAACACC
	SO_4230D2	TTAAGAACGGGTTCTTGCTACTGCGGCCACCACATATTTCTTTTGCAC
	SO_4230D3	GTGCAAAAGAAATATGTGGTGGCCGCAGTAGCAAGAACCCGTTCTTAA
	SO_4230D4SalI	GACT<u>GTCGAC</u>GGAATTAGCCTGAGTTACCAGC
	SO_4230TR	CCTGTATGACATCAACCATCAGC
SO_0900 (cloning)	SO_0900_pQEfwd	GACT<u>GGATCC</u>ATGGAATACAGACGCATACCGC
	SO_0900_pQErev	GACT<u>GTCGAC</u>CTAAGGACAGGGCAATCTAAATTG
SO_4673 (cloning)	SO_4673_pQEfwd	GACT<u>GGATCC</u>ATGAAAGCACTAAGCAAGTTAAAAGC
	SO_4673_pQErev	GACT<u>GTCGAC</u>TTAATCCCAGCTGAGGATGACTTTACC
SO_4230 (cloning)	SO_4230_pQEfwd	GACT<u>GGATCC</u>GTGCAAAAGAAATATGTGGTGGCCC
	SO_4230_pQErev	GACT<u>GGTACC</u>TTAAGAACGGGTTCTTGCTACTGC
SO_1396[Q207H] (cloning)	SO_1396_pBBRfwd	CTCGCA<u>GGATCC</u>GCTAAGGAGACGAGAAATTGGGGATATTTTTTA TGAATATC
	SO_1396_pBBRrev	CGATGC<u>GTCGAC</u>TCAGTATTTTGAAGCTTGCTGGCG
SO_2452 (cloning)	SO_2452_pQEfwd	CATGAT<u>GGATCC</u> ATGGAGCAACATCAAGTTTGG
	SO_2452_pQErev	TCCATC<u>GTCGAC</u> ATCTATCACTCGTTTAGGGTTAACACT

[a] Underline indicates restriction enzyme cutting site.

measuring the catalytic activity of xylose reductase on xylose, K_m and V_{max} were determined by varying the xylose concentrations (0.01 to 0.25 M) under constant concentrations of NADPH (0.35 mM) and purified protein (10 μl) in the assay mixture and fitting the data to the Lineweaver-Burk equation: $1/V = (K_m/V_{max})[S] + 1/V_{max}$, where V is the reaction rate and S is the substrate concentration. The extinction coefficient (ε) for NADPH at 340 nm is 6.22×10^{-3} M^{-1} cm^{-1}. One unit of xylose reductase activity is the amount of enzyme which converts 1 μmol of NADPH to NADP$^+$ per min. Xylulokinase was assayed by previously described methods (33). Reactions were carried out at 30°C and pH 7.5 in 96-well microtiter plates in a final volume of 200 μl. The reaction mixture consisted of the following (final concentrations indicated): 71 mM Tris-HCl (pH 7.5), 7.1 mM MgCl$_2$, 1 mM EDTA, 50 mM KCl, 7.1 mM KF, 5 mM KCN, 1.4 mM ATP, 1 mM phosphoenolpyruvate (PEP), 0.3 mM NADH, 0.7 U ml^{-1} of pyruvate kinase, 1 U ml^{-1} of lactate dehydrogenase, and 5 mM xylulose. NADH consumption was monitored continuously at 340 nm for 10 min. One unit of xylulokinase activity is the amount of enzyme that converts 1 μmol of NADH to NAD$^+$ per min. For measuring the catalytic activity of xylulokinase on xylulose, K_m and V_{max} were determined by varying the xylulose concentrations (1 to 20 mM) under constant concentrations of NADH (0.3 mM) and purified protein (10 μl) in the assay mixture. Xylitol dehydrogenase (XDH) was assayed by a previously described method (34); the reaction mixture consisted of (final concentrations indicated) 77 mM glycine, 6.3 mM NAD$^+$, 1 mM 2-mercaptoethanol, and 200 mM xylitol. The consumption of NADH was monitored continuously at 340 nm for 10 min. One unit of xylitol dehydrogenase activity is the amount of enzyme that converts 1 μmol of NAD$^+$ to NADH per min. For measuring the catalytic activity of xylitol

dehydrogenase on xylitol, K_m and V_{max} were determined by varying the xylitol concentrations (1 to 200 mM) under constant concentrations of NAD$^+$ (6.3 mM) and purified protein (10 μl) in the assay mixture.

In-frame deletion mutagenesis of *S. oneidensis* genes SO_1396[Q207H], SO_0900, and SO_4230. Genes encoding SO_1396[Q207H], SO_0900, and SO_4230 were deleted in frame from the XM1 genome as described previously (35). Regions corresponding to ~750 bp upstream and downstream of each open reading frame (ORF) were PCR amplified with iProof ultrahigh-fidelity polymerase (Bio-Rad, Hercules, CA), generating fragments F1 and F2, which were fused by overlap extension PCR to generate fragment F3. The primers used for construction of ΔSO1396[Q207H], ΔSO0900, and ΔSO4230 strains are listed in Table 3. Fragment F3 was cloned into pKO2.0 with BamHI and SalI restriction endonucleases and electroporated into *E. coli* strain β2155 λ *pir*. pKO2.0-F3 was mobilized into recipient wild-type *S. oneidensis* via biparental mating procedures. A plasmid integrant was identified via PCR analysis, and the mutation was resolved on LB agar containing sucrose (10%). Following counterselection on LB agar containing sucrose (10% [wt/vol]), the corresponding in-frame deletion mutant strains (designated XM1-ΔSO1396[Q207H], XM1-ΔSO0900, and XM1-ΔSO4230, respectively) were isolated and confirmed via PCR and sequencing of the DNA fragments. The *S. oneidensis* wild type, XM1, and the ΔSO1396[Q207H], ΔSO0900, and ΔSO4230 mutants were tested for aerobic growth with 5 mM xylose as the electron donor and O$_2$ as the terminal electron acceptor. The cells were incubated at 30°C for 144 h, and samples were withdrawn periodically for determination of cell density (OD$_{600}$).

Homology modeling and amino acid sequence analysis of SO_1396[Q207H]. The secondary structure of SO_1396[Q207H] was predicted using the I-TASSER server, and a model structure was constructed based
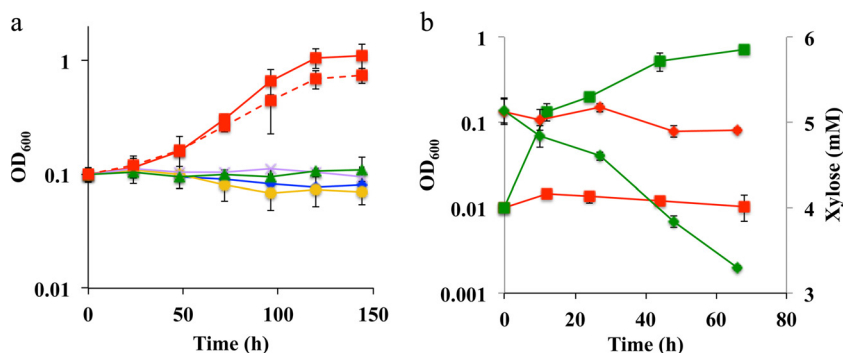
FIG 2 Aerobic growth profiles of *S. oneidensis* and strain XM1 strains in the presence of xylose as the sole carbon and electron source in minimal medium. Xylose at 5 mM was used in this experiment. (a) Initial $OD_{600} = 0.1$. Blue diamonds, wild type; red squares with solid line, XM1; orange circles, XM1-ΔSO1396^{Q207H}; red squares with dashed line, XM1-ΔSO1396^{Q207H} + pBBR_SO_1396^{Q207H}; violet crosses, XM1-ΔSO0900; green triangles, XM1-ΔSO4230. Error bars represent ranges of errors in duplicate batch reactors. (b) Growth and xylose concentration profiles of *S. oneidensis* and strain XM1 in the presence of O_2 as the electron acceptor in minimal medium. Initial $OD_{600} = 0.01$. Red shapes, wild type; green shapes, XM1; squares, OD_{600}; diamonds, xylose concentration.

on secondary structure similarity to known protein structures in the protein database. The membrane domain of the respiratory complex I from *E. coli* (PDB code: 3RKO, chain C [3rkoC]) was used as the template to construct SO_1396^{Q207H} models based on the best Z-scores with known protein structures by I-TASSER (31). SO_1396 homologs in the NCBI databases were identified via BLAST analysis using SO_1396 of wild-type *S. oniedensis* as the search query. Multiple alignments of wild-type SO_1396 homologs were generated with ClustalW (http://www.ebi.ac.uk/Tools/clustalw2/index.html) (36).

Cloning and expression of SO_1396^{Q207H} in *S. oneidensis*. The primers used for cloning SO_1396^{Q207H} on pBBR1MCS are listed in Table 3. The cloned plasmid was transformed into strain XM1-ΔSO1396^{Q207H}. The resulting recombinant strain was cultured in LB medium with 25 µg ml^{-1} of chloramphenicol. Strain XM1-ΔSO1396^{Q207H} pBBR1MCS + SO_1396^{Q207H} was tested for aerobic growth with 5 mM xylose as the electron donor 30°C for 144 h, and samples were withdrawn periodically for determination of cell density (OD_{600}).

Analytical methods. The concentration of reducing ends of the supernatant was determined by the dinitrosalicylic acid (DNS) assay (29). One hundred microliters of the supernatant was added to 900 µl of DNS solution prepared by dissolving in water a mixture of 0.75% 3,5-dinitrosalicylic acid, 1.4% sodium hydroxide, 21.6% potassium sodium tartrate, 0.55% phenol, and 0.55% sodium metabisulfate. The mixture was then boiled for 5 min and centrifuged at 15,000 × *g* for 5 min, and the absorbance of the supernatant was measured at 545 nm. Reducing sugar concentrations were calculated using glucose as a standard.

Xylose concentrations were measured via high-pressure liquid chromatography (HPLC) by following a modified version of a previously described protocol (37). Three hundred microliters of xylose solution was mixed with 100 µl of 1.4 M sodium cyanoborohydride solution in water, 700 µl of a methanolic solution of 0.6 M aminobenzoic butyl ester (ABBE), and 100 µl of 10% acetic acid. The solution was heated at 80°C for 60 min and then extracted three times with 0.5 ml of dichloromethane prior to injection directly into the HPLC system equipped with a SUPELCOSIL LC-18-DB column. The mobile phase was comprised of 0.1 M ammonium acetate, pH 4.5 (solvent A), and acetonitrile (solvent B). Separation was carried out with a mixture of mobile phase A-acetonitrile (75:25 [vol/vol]) at a flow rate of 0.5 ml/min. Chromatograms were generated at 260 nm, and a calibration curve was generated from a standard. Nitrite (NO_2^-) concentrations were measured by diluting samples 250-fold in a solution consisting of 9.6 mM sulfanilic acid, 96 mM potassium bisulfate, and 3.2 mM *N,N*-ethylenediamine (38). Samples were held in the dark for 15 min prior to measuring absorbance at 510 nm.

Protein concentrations were measured by the Bradford assay using a protein reagent dye (Bio-Rad, Hercules, CA) with bovine serine albumin

as the standard. SDS-PAGE was performed using a Mini-protean TGX electrophoresis kit (Bio-Rad) and stained with Bio-safe Coomassie blue (Bio-Rad). A 100-kDa Precision Plus Protein standard ladder was used as a standard mass protein marker. Cell density (OD_{600}) was measured on a UV-visible light spectrophotometer (Beckman Coulter, CA).

RESULTS

Isolation of xylose-adapted *S. oneidensis* strain XM1. Wild-type *S. oneidensis* is unable to grow with xylose as the carbon and energy source. The wild-type strain was therefore subjected to an adaptive evolution strategy to generate *S. oneidensis* mutants with the acquired ability to metabolize xylose as the carbon and energy source. Wild-type *S. oneidensis* cells were initially grown in SM minimal growth medium with 18 mM lactate as the carbon and energy source and subsequently serially transferred over a 12-month period to SM medium amended with increasing ratios of xylose to lactate concentrations (Table 2). *S. oneidensis* strain XM1 was isolated from the adaptively evolved mutant mix after the 12th successive transfer. Strain XM1 grew aerobically with 65 mM xylose as the sole carbon and energy source. However, strain XM1 was unable to grow aerobically on a variety of other sugars, including glucose, arabinose, galactose, lactose, sucrose, cellobiose, fructose, maltose, mannose, mannitol, trehalose, xylitol, and gluconate (data not shown). This finding suggests that strain XM1 may have developed a GASP phenotype specific to xylose. Similar findings were previously reported with *S. oneidensis* mutants adapted to grow in the presence of glucose as the carbon and energy source (15).

Rates of xylose consumption by xylose-adapted *S. oneidensis* strain XM1. Strain XM1 was further tested for xylose consumption in SM minimal medium amended with 5 mM xylose as the carbon and energy source. Under aerobic conditions, strain XM1 grew at a rate of 0.063 h^{-1} (Fig. 2b), while the wild-type strain grew at a rate of 0.003 h^{-1} (i.e., at 5% of the rate of strain XM1). Strain XM1 consumed xylose at a rate of 27 µM h^{-1}, while the wild-type strain consumed xylose at a rate of 1.2 µM h^{-1} (i.e., 5% of the rate of strain XM1) (Fig. 2b). Strain XM1 was also able to utilize lactate as the sole carbon source at a rate similar to that of the wild-type strain, thus indicating that lactate metabolism was not altered during the adaptation process (data not shown). The anaerobic respiratory capabilities of the *S. oneidensis* wild type and

strain XM1 were also determined under anaerobic conditions with xylose as the electron donor and NO_3^-, fumarate, or Fe(III) as the electron acceptor.

With NO_3^- as the electron acceptor, strain XM1 grew at the rate of $0.027 \, h^{-1}$ (see Fig. S4b in the supplemental material), while the wild-type strain grew at a much lower rate, $0.002 \, h^{-1}$ (i.e., 7% of the rate of strain XM1). Strain XM1 consumed xylose at a rate of $6.32 \, \mu M \, h^{-1}$, while the wild-type strain consumed xylose at $1.9 \, \mu M \, h^{-1}$ (i.e., at 30% of the rate of strain XM1) (see Fig. S4b). Strain XM1 produced nitrite (product of microbially catalyzed nitrate reduction) at the rate of $38.2 \, \mu M \, h^{-1}$ (see Fig. S4c), while the wild-type strain produced nitrite at a much lower rate, $1.5 \, \mu M \, h^{-1}$ (i.e., at 4% of the rate of strain XM1). With fumarate as the electron acceptor, strain XM1 grew at the rate of $0.034 \, h^{-1}$ (see Fig. S4a), while the wild-type strain grew at a rate of $0.002 \, h^{-1}$ (i.e., at 6% of the rate of strain XM1). Strain XM1 consumed xylose at a rate of $10.6 \, \mu M \, h^{-1}$, while the wild-type strain consumed xylose at $0.73 \, \mu M \, h^{-1}$ (i.e., at 7% of the rate of strain XM1) (see Fig. S4a). With Fe(III) as the electron acceptor, strain XM1 produced Fe(II) [product of microbially catalyzed Fe(III) reduction] at the rate of $20.9 \, \mu M \, h^{-1}$) (see Fig. S4d), while the wild-type strain produced Fe(II) at a much lower rate, $3.0 \, \mu M \, h^{-1}$ (i.e., at 14% of the rate of strain XM1). During the 68-h growth period, strain XM1 consumed xylose at a rate of $6.8 \, \mu M \, h^{-1}$, while the wild-type strain consumed xylose at $2.2 \, \mu M \, h^{-1}$ (i.e., at 32% of the rate of strain XM1) (see Fig. S4d). These results indicate that strain XM1 consumed xylose under aerobic and anaerobic nitrate-, fumarate-, and Fe(III)-reducing conditions.

Identification of the xylose transporter in *S. oneidensis*. The single nucleotide mutation that enabled strain XM1 to grow on xylose as the carbon and energy source was identified by whole-genome sequencing. A single nucleotide mutation was identified in SO_1396 that converted glutamine (Q) to histidine (H) at amino acid position 207. Mutations were not found elsewhere in the SO_1396 gene or in other genes in strain XM1. SO_1396 is annotated as a membrane protein of unknown function (30). To investigate the function of SO_1396^{Q207H} in strain XM1, in-frame gene deletion mutant XM1-ΔSO1396^{Q207H} was tested for the ability to metabolize xylose as the sole carbon and energy source under aerobic conditions. Strain XM1 grew at the rate of $0.035 \, h^{-1}$, while strain XM1-ΔSO1396^{Q207H} was unable to grow in the presence of xylose as the sole carbon and energy source (Fig. 2a). Expression of SO_1396^{Q207H} on plasmid pBBR1MCS in the XM1-ΔSO1396^{Q207H} strain rescued the growth on xylose by approximately 84% (with a growth rate of $0.029 \, h^{-1}$ [Fig. 2a]). These results suggest that the mutant membrane protein SO_1396^{Q207H} functions as a xylose transporter. Homology modeling of SO_1396^{Q207H} (Fig. 3a) predicted that the secondary structure of SO_1396^{Q207H} is partly outward occluded, with a top width of 62 Å and a bottom width of 53 Å. Only minor secondary-structure changes were observed in overlapping structures of SO_1396^{Q207} and SO_1396^{Q207H} (Fig. 3b and c).

Identification of genes encoding the xylose metabolic pathway of strain XM1. Strain XM1 containing mutated membrane protein SO_1396^{Q207H} consumed xylose as the carbon and energy source under both aerobic and anaerobic conditions. To identify the genes encoding the xylose metabolic pathway, proteins similar to known xylose metabolic proteins in other organisms were identified in the XM1 genome sequence via BLAST sequence analysis (30). Xylose isomerase and all proteins involved in the Weimberg-

Dahms pathway were absent from the strain XM1 genome (data not shown). For the oxidoreductase pathway, the aldo/keto reductase SO_0900 in the strain XM1 genome displayed significant identity to known xylose reductases in *E. coli* (31% identical to ECs0473) and *Z. mobilis* (32% identical to ZMO0976) (see Table S2 in the supplemental material) (32). SO_0900 was therefore hypothesized to function as the xylose reductase (XR) in strain XM1.

D-Xylitol dehydrogenase (XDH) is the next protein following xylose reductase in the oxidoreductase pathway. XDH is a member of the alcohol and threonine dehydrogenase protein superfamily, containing NAD(P) and catalytic zinc binding domains for conversion of xylitol to xylulose (39). L-Threonine dehydrogenase SO_4673 displayed significant identity to xylitol dehydrogenase (20 to 28% [see Table S3 in the supplemental material]) and also contains NAD(P) and catalytic zinc binding domains (30). Alcohol dehydrogenase SO_2452 displayed 21 to 22% identity to known D-xylitol dehydrogenases (see Table S4). In addition, *S. halifaxis* and *S. pealeana* metabolize xylitol and contain an alcohol dehydrogenase that functions as xylitol dehydrogenase (18). SO_4673 and SO_2452 were therefore targeted as candidates for xylitol dehydrogenase in strain XM1.

Xylulokinase (XK) is the next protein following D-xylitol dehydrogenase in the oxidoreductase pathway. XK displayed significant identity (24 to 28% [see Table S5 in the supplemental material) to SO_4230, a glycerol kinase (GlpK). Based on secondary-structure alignment, *E. coli* GlpK is highly identical to xylulokinase in *E. coli* (40). Since GlpK proteins from strain XM1 and *E. coli* display 72% identity (see Table S5), SO_4230 was predicted to function as the xylulokinase in strain XM1. The proteins following xylulokinase in the known xylose metabolic pathway are present in the XM1 genome (41).

Purification and activity of xylose metabolic pathway proteins in strain XM1. Based on BLAST identities, strain XM1 proteins SO_0900, SO_4673, SO_2452, and SO_4230 were predicted to be involved in the xylose metabolic pathway. The corresponding genes were cloned into expression vector pQE80L and transformed into *E. coli* JM109. The enzymes were expressed as fusion proteins with a His tag at their N termini, and one-step affinity purification was based on the interaction of the N-terminal His tag and nickel affinity gel. The purified proteins SO_0900, SO_4673, SO_2452, and SO_4230 displayed the expected molecular masses of ~41, 41, 38, and 60 kDa on SDS-PAGE gels (see Fig. S1 and S2 in the supplemental material). Purified SO_0900 displayed XR specific activity of 2.93 U/mg, with a V_{max} of 3.41 U/mg and K_m of 93 mM, with 250 mM xylose as the substrate (Table 4). Purified SO_4230 displayed XK specific activity of 0.2 U/mg, with a V_{max} of 0.52 U/mg and K_m of 1.7 mM, with 5 mM xylulose as the substrate (Table 4). However, purified proteins SO_4673 and SO_2452 did not display XDH activity with various levels of xylitol (1 to 200 mM) as the substrate. These results indicate that SO_0900 and SO_4230 may function as the xylose reductase and xylulokinase, respectively. However, the identity of XDH in strain XM1 remains unknown. To confirm the role of SO_0900 and SO_4230 in the xylose metabolism in strain XM1, SO_0900 and SO_4230 were deleted in frame and the resulting single-gene-knockout mutants (strains XM1-Δ0900 and XM1-Δ4230) were tested for the ability to utilize xylose as the carbon and energy source under aerobic conditions. Strain XM1 grew at the rate of $0.035 \, h^{-1}$, while strains XM1-Δ0900 and XM1-Δ4230 were unable to grow in the presence
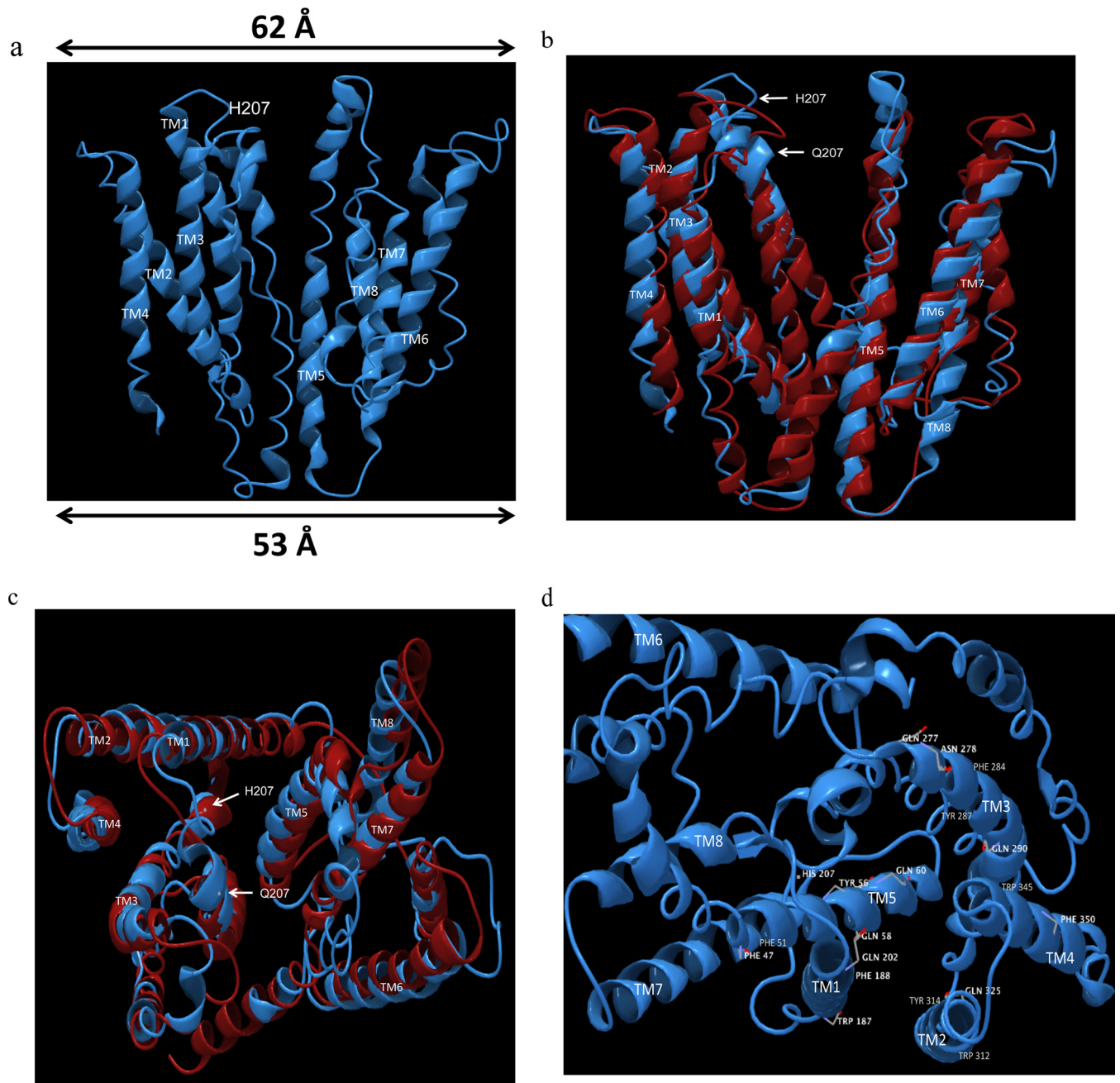
FIG 3 Predicted secondary structure of SO_1396^{Q207H}. (a) The homology model based on membrane domain of the respiratory complex I from *E. coli* as the template (PDB code: 3rkoC) contains 8 transmembrane domains (labeled as TM). A single point mutation in xylose-adapted XM1 was found in SO_1396 at the 207th amino acid residue (Q207H). (b) Front view of secondary structure alignment between WT SO_1396 and SO_1396^{Q207H}. Red, WT SO_1396; blue, SO_1396^{Q207H}. (c) Top view of secondary-structure alignment between WT SO_1396 and SO_1396^{Q207H}. Red, WT SO_1396; blue, SO_1396^{Q207H}. (d) Top view of homology model of SO_1396^{Q207H} illustrating the residues predicted to aid in xylose binding and uptake.

of xylose as the carbon and energy source (Fig. 2a). These results suggest that SO_0900 and SO_4230 function as the xylose reductase and xylulokinase, respectively, in strain XM1.

DISCUSSION

The facultative anaerobe *S. oneidensis* respires a diverse spectrum of electron acceptors under both aerobic and anaerobic conditions (14, 42, 43). *S. oneidensis* is employed to drive electricity

production in microbial fuel cells and to produce the biofuels ethanol and isobutanol from substrates such as glycerol and glucose through metabolic engineering (16, 17, 44). However, *S. oneidensis* displays a more limited range of electron donor utilization (13, 44). Electron-rich carbon sources such as glucose and xylose are the primary products derived from the saccharification of lignocellulosic biomass (45). Recently, *S. oneidensis* was adaptively evolved and metabolically engineered to metabolize glucose as the

TABLE 4 Kinetic parameters of purified proteins in this study[a]

Protein	Substrate	Enzyme activity assay	Sp act (U/mg)	V_{max} (U/mg)	K_m (mM)
SO_0900	Xylose	Xylose reductase	2.93 ± 0.17 (250 mM)	3.41 ± 0.21	93 ± 7
SO_4230	Xylulose	Xylulokinase	0.2 ± 0.013 (5 mM)	0.52 ± 0.02	1.7 ± 0.12
SO_4673	Xylitol	Xylitol dehydrogenase	ND[b]	ND	ND
SO_2452	Xylitol	Xylitol dehydrogenase	ND	ND	ND

[a] Error values represent range of errors in duplicate samples. Substrate concentrations are given in parentheses for respective specific activities.
[b] ND, not detectable.

carbon and energy source (15–17). Although the complete glucose metabolic pathway has been identified in *S. oneidensis*, xylose metabolism remains elusive (18). The present study is the first report to identify a previously unknown xylose catabolic pathway in *S. oneidensis*.

Xylose catabolic pathways were not previously detected in the *S. oneidensis* genome (18), and correspondingly, wild-type *S. oneidensis* was unable to consume xylose (Fig. 2; see also Fig. S4 in the supplemental material). The newly isolated, xylose-adapted strain XM1, on the other hand, consumed xylose and grew under aerobic and anaerobic nitrate-, fumarate-, and Fe(III)-reducing conditions (Fig. 2; see also Fig. S4). Whole-genome sequencing indicated that strain XM1 contained a mutation in unknown membrane protein SO_1396, resulting in a glutamine-to-histidine conversion at amino acid position 207. BLAST analysis indicated that SO_1396 homologs with unknown function (40 to 95% identity [see Table S7]) were present in the genomes of 14 other *Shewanella* species. None of the SO_1396 homologs contain histidine at position 207, thus indicating that the silent SO_1396 xylose transporter is not confined to only *S. oneidensis* MR-1 but is widespread throughout the *Shewanella* genus.

Only minor structural differences were noted between the predicted structures of SO_1396 wild-type and Q207H mutant forms (Fig. 3b and c). Histidine is weakly charged at circumneutral pH with the bulky (imidazole) R-group pK_a of 6.0, while glutamine is polar and neutral at pH 7.0. Multiple-sequence alignment of SO_1396 homologs of 14 sequenced *Shewanella* genomes revealed that the most commonly found amino acid residues at position 207 of SO_1396 were glutamine, arginine, and lysine (all containing an amine group side chain [Fig. 4; see also Fig. S6 in the supplemental material]). The amino acid distribution bracketing position 207 of SO_1396 across all *Shewanella* SO_1396 homologs is

highly variable (Fig. 4; see also Fig. S6). The structural change caused by replacement of glutamine with the imidazole structure of histidine in SO_1396[Q207H] is predicted to facilitate transport of xylose into strain XM1 by SO_1396[Q207H] via interaction with predicted active-site residues. Similar point mutations alter substrate specificities in a variety of other sugar transporters (46–48). The SO_1396[Q207H] structure is predicted to contain 8 transmembrane domains (TM) (Fig. 3), and the structure is outward occluded, with the top wider (62 Å) than the bottom (53 Å), which is similar to the dimensions of *E. coli* xylose transporter XylE (29% sequence identity [Table 5]). The predicted structure of SO_1396[Q207H] is based on the structure of *E. coli* respiratory complex I (PDB code: 3rkoC) (Fig. 3). Xylose transport by XylE is coordinated through hydrogen bonding by glutamine and asparagine and interaction with several aromatic amino acid residues (tyrosine, tryptophan, and phenylalanine) (49). Similar polar residues found in SO_1396[Q207H] included Q202 (TM5), Q277 (TM6), Q290 (TM6), Q325 (TM7), and N278 (TM6), and aromatic residues included W187 (TM5), W312 (TM7), W345 (TM8), Y287 (TM6), Y314 (TM7), F188 (TM5), F284 (TM6), and F350 (TM8). These residues may play a similar role by aiding xylose binding and uptake by SO_1396[Q207H] (Fig. 3d).

Strain XM1 is predicted to contain the xylose oxidoreductase pathway (Fig. 1). Although the XM1 genome does not contain a putative xylose reductase, the aldo/keto reductase SO_0900 displayed significant identity to the *E. coli* and *Z. mobilis* xylose reductases (see Table S2 in the supplemental material) (32). The kinetic parameters of XR activity of purified SO_0900 with xylose as the substrate were comparable to those of ZMO0976 from *Z. mobilis* (see Table S6). Moreover, deletion mutant XM1-ΔSO0900 was unable to metabolize xylose as the carbon and energy source,
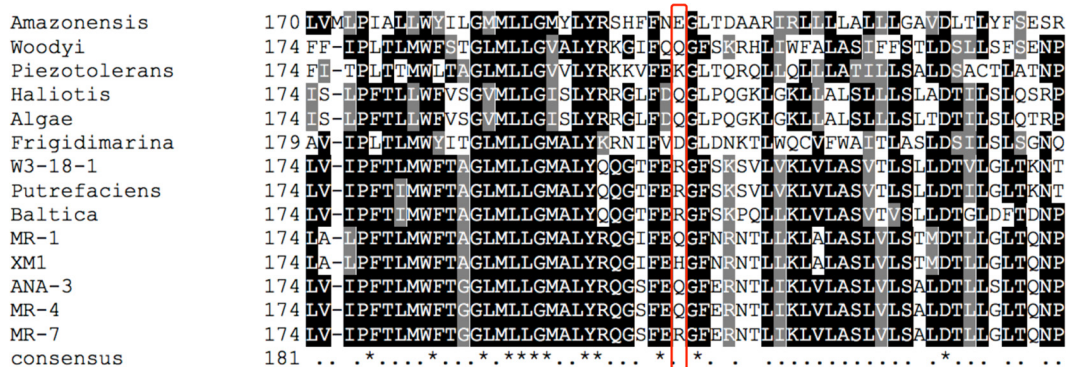

FIG 4 Multiple-sequence alignments generated by ClustalW analysis of *S. oneidensis* MR-1 SO_1396 homologs identified in the genomes of 14 *Shewanella* strains. Black shading indicates identity and gray shading indicates similarity. The red box indicates position 207 of SO_1396 across all 14 *Shewanella* SO_1396 homologs.

TABLE 5 BLAST analysis of SO_1396^{Q207H}

Parameter	Protein/locus tag	Organism	Size (aa^a)	Identity (%)	Similarity (%)	E value	Coverage (%)	Function
	SO_1396^{Q207H} (template)	XM1	365					Membrane protein of unknown function
Top 3 hits in *Shewanella*	Sbal223_1289	*S. baltica* OS223	401	78	88	0	99	Protein of unknown function
	AEA42_07100	*Shewanella* sp. Sh95	400	86	94	0	96	Hypothetical protein
	WP_055647337	*Shewanella* sp. ZOR0012	400	86	93	0	96	Hypothetical protein
Top 3 hits outside *Shewanella*	BG00_17450	*Pseudoalteromonas* sp. SCSIO_11900	361	40	61	3.E−79	95	Hypothetical protein
	AMS57_07405	*Pseudoalteromonas tetraodonis*	361	40	61	4.E−78	95	Hypothetical protein
	ND6B_3400	*Pseudoalteromonas* sp. ND6B	366	40	61	5.E−78	95	Hypothetical protein
Known D-xylose transporter	XylE	*E. coli*	491	29	51	2.E−02	60	D-Xylose MFS transporter

^{a} aa, amino acids.

thus indicating that SO_0900 may function as a xylose reductase (Fig. 2a).

The secondary structure of *E. coli* GlpK is homologous to that of *E. coli* XK, and the kinetic and structural properties of *E. coli* XK are derived from *E. coli* GlpK (40). Interestingly, XM1 GlpK (SO_4230) was also highly identical (72% [see Table S5]) to *E. coli* GlpK, and the secondary structure of the SO_4230 protein was highly homologous to that of *E. coli* XK (see Fig. S3). Moreover, residues Asp10 and Asp244 (required for XK catalytic activity in *E. coli*) of SO_4230 were homologous to Asp6 and Asp233 of *E. coli* XK, respectively (highlighted in green in Fig. S3 in the supplemental material) (40). SO_4230 displayed XR activity with D-xylulose as the substrate; however, unlike for SO_0900, the kinetic parameters of SO_4230 differed from those of other known XKs (see Table S6). The specific activity and V_{max} of known XKs were up to 100-fold higher than those of SO_4230. The K_m of SO_4230 was 3- to 5-fold higher than that of known XKs (see Table S6). Deletion mutant strain XM1-ΔSO4230 was unable to metabolize xylose as the carbon and energy source, thus indicating that SO_4230 may function as a xylulokinase (Fig. 2a).

Although SO_4673 and SO_2452 displayed significant identities to known XDH proteins (see Tables S3 and S4), purified forms of SO_4673 and SO_2452 did not display XDH activity with D-xylitol as the substrate (Table 4). However, SO_4673 and SO_2452 displayed dehydrogenase activity with threonine and ethanol as the substrates, respectively (data not shown), thus confirming that the purified proteins were active. The current working model of the xylose catabolic pathway in strain XM1 includes putative xylose transporter SO_1396^{Q207H}, xylose reductase SO_0900, and xylulose reductase SO_4230 identified in the present study (see Fig. S5). The identity of *S. oneidensis* XDH, however, remains unknown.

An otherwise silent xylose catabolic pathway was activated in *S. oneidensis* by application of an adaptive evolution strategy. The expansion of *S. oneidensis* to metabolize the lignocellulose component xylose is an example of how accidental mutations allow microorganisms to adaptively evolve. The expansion of the *S. oneidensis* metabolic repertoire to xylose expands the electron donors whose oxidation may be coupled to the myriad of terminal electron-accepting processes catalyzed by *S. oneidensis*. Since xylose is a lignocellulose degradation product, this study expands the potential substrates to include lignocellulosic biomass. Metabolism of multiple carbon sources, such as glucose, glycerol, and xylose, by *S. oneidensis* has the potential to improve the efficiency of electricity generation, biofuel production, and bioremediation of toxic contaminants (16, 17, 50).

REFERENCES

1. **Jackson S, Nicolson SW.** 2002. Xylose as a nectar sugar: from biochemistry to ecology. Comp Biochem Physiol B Biochem Mol Biol **131**:613–620. http://dx.doi.org/10.1016/S1096-4959(02)00028-3.
2. **Lia X, Parka A, Estrelaa R, Kimb S, Jin Y, Cate J.** 2016. Comparison of xylose fermentation by two high-performance engineered strains of *Saccharomyces cerevisiae*. Biotechnol Rep **9**:53–56. http://dx.doi.org/10.1016/j.btre.2016.01.003.
3. **Li P, Sun H, Chen Z, Li Y, Zhu T.** 2015. Construction of efficient xylose utilizing *Pichia pastoris* for industrial enzyme production. Microb Cell Fact **14**:22. http://dx.doi.org/10.1186/s12934-015-0206-8.
4. **Lee SJ, Lee SJ, Lee DW.** 2013. Design and development of synthetic microbial platform cells for bioenergy. Front Microbiol **4**:92. http://dx.doi.org/10.3389/fmicb.2013.00092.
5. **Sandström AG, Munoz de Las Heras A, Portugal-Nunes D, Gorwa-Grauslund MF.** 2015. Engineering of *Saccharomyces cerevisiae* for the production of poly-3-D-hydroxybutyrate from xylose. AMB Express **5**:14. http://dx.doi.org/10.1186/s13568-015-0100-0.
6. **Agrawal M, Mao ZC, Chen RR.** 2011. Adaptation yields a highly efficient xylose-fermenting *Zymomonas mobilis* strain. Biotechnol Bioeng **108**:777–785. http://dx.doi.org/10.1002/bit.23021.
7. **Ko BS, Kim J, Kim JH.** 2006. Production of xylitol from D-xylose by a xylitol dehydrogenase gene-disrupted mutant of *Candida tropicalis*. Appl Environ Microbiol **72**:4207–4213. http://dx.doi.org/10.1128/AEM.02699-05.
8. **Stephens C, Christen B, Fuchs T, Sundaram V, Watanabe K, Jenal U.** 2007. Genetic analysis of a novel pathway for D-xylose metabolism in *Caulobacter crescentus*. J Bacteriol **189**:2181–2185. http://dx.doi.org/10.1128/JB.01438-06.
9. **Young E, Poucher A, Comer A, Bailey A, Alper H.** 2011. Functional survey for heterologous sugar transport proteins, using *Saccharomyces cerevisiae* as a host. Appl Environ Microbiol **77**:3311–3319. http://dx.doi.org/10.1128/AEM.02651-10.
10. **Gu Y, Ding Y, Ren C, Sun Z, Rodionov DA, Zhang W, Yang S, Yang C, Jiang W.** 2010. Reconstruction of xylose utilization pathway and regulons in *Firmicutes*. BMC Genomics **11**:255. http://dx.doi.org/10.1186/1471-2164-11-255.
11. **Ceroni F, Carbonell P, Francois JM, Haynes KA.** 2015. Editorial—synthetic biology: engineering complexity and refactoring cell capabilities. Front Bioeng Biotechnol **3**:120. http://dx.doi.org/10.3389/fbioe.2015.00120.
12. **Lee SM, Jellison T, Alper HS.** 2012. Directed evolution of xylose isomerase for improved xylose catabolism and fermentation in the yeast *Saccharomyces cerevisiae*. Appl Environ Microbiol **78**:5708–5716. http://dx.doi.org/10.1128/AEM.01419-12.

13. **Szeinbaum N, Burns JL, DiChristina TJ.** 2014. Electron transport and protein secretion pathways involved in Mn(III) reduction by *Shewanella oneidensis*. Environ Microbiol Rep **6**:490–500. http://dx.doi.org/10.1111/1758-2229.12173.

14. **Wee SK, Burns JL, DiChristina TJ.** 2014. Identification of a molecular signature unique to metal-reducing *Gammaproteobacteria*. FEMS Microbiol Lett **350**:90–99. http://dx.doi.org/10.1111/1574-6968.12304.

15. **Howard EC, Hamdan LJ, Lizewski SE, Ringeisen BR.** 2012. High frequency of glucose-utilizing mutants in *Shewanella oneidensis* MR-1. FEMS Microbiol Lett **327**:9–14. http://dx.doi.org/10.1111/j.1574-6968.2011.02450.x.

16. **Choi D, Lee SB, Kim S, Min B, Choi IG, Chang IS.** 2014. Metabolically engineered glucose-utilizing *Shewanella* strains under anaerobic conditions. Bioresour Technol **154**:59–66. http://dx.doi.org/10.1016/j.biortech.2013.12.025.

17. **Flynn JM, Ross DE, Hunt KA, Bond DR, Gralnick JA.** 2010. Enabling unbalanced fermentations by using engineered electrode-interfaced bacteria. mBio **1**:e00190-10. http://dx.doi.org/10.1128/mBio.00190-10.

18. **Rodionov DA, Yang C, Li X, Rodionova IA, Wang Y, Obraztsova AY, Zagnitko OP, Overbeek R, Romine MF, Reed S, Fredrickson JK, Nealson KH, Osterman AL.** 2010. Genomic encyclopedia of sugar utilization pathways in the *Shewanella* genus. BMC Genomics **11**:494. http://dx.doi.org/10.1186/1471-2164-11-494.

19. **Roth JR, Kugelberg E, Reams AB, Kofoid E, Andersson DI.** 2006. Origin of mutations under selection: the adaptive mutation controversy. Annu Rev Microbiol **60**:477–501. http://dx.doi.org/10.1146/annurev.micro.60.080805.142045.

20. **Finkel SE.** 2006. Long-term survival during stationary phase: evolution and the GASP phenotype. Nat Rev Microbiol **4**:113–120. http://dx.doi.org/10.1038/nrmicro1340.

21. **Fong SS, Marciniak JY, Palsson BO.** 2003. Description and interpretation of adaptive evolution of *Escherichia coli* K-12 MG1655 by using a genome-scale in silico metabolic model. J Bacteriol **185**:6400–6408. http://dx.doi.org/10.1128/JB.185.21.6400-6408.2003.

22. **Kuyper M, Toirkens MJ, Diderich JA, Winkler AA, van Dijken JP, Pronk JT.** 2005. Evolutionary engineering of mixed-sugar utilization by a xylose-fermenting *Saccharomyces cerevisiae* strain. FEMS Yeast Res **5**:925–934. http://dx.doi.org/10.1016/j.femsyr.2005.04.004.

23. **Rosenberg SM.** 2001. Evolving responsively: adaptive mutation. Nat Rev Genet **2**:504–515. http://dx.doi.org/10.1038/35080556.

24. **Tang YJ, Martin HG, Dehal PS, Deutschbauer A, Llora X, Meadows A, Arkin A, Keasling JD.** 2009. Metabolic flux analysis of *Shewanella* spp. reveals evolutionary robustness in central carbon metabolism. Biotechnol Bioeng **102**:1161–1169. http://dx.doi.org/10.1002/bit.22129.

25. **Sambrook J, Fritsch EF, Maniatis T.** 1989. Molecular cloning: a laboratory manual, 2nd ed. Cold Spring Harbor Laboratory Press, Cold Spring Harbor, NY.

26. **DiChristina TJ, DeLong EF.** 1994. Isolation of anaerobic respiratory mutants of *Shewanella putrefaciens* and genetic analysis of mutants deficient in anaerobic growth on Fe^{3+}. J Bacteriol **176**:1468–1474.

27. **Taratus EM, Eubanks SG, DiChristina TJ.** 2000. Design and application of a rapid screening technique for isolation of selenite reduction-deficient mutants of *Shewanella putrefaciens*. Microbiol Res **155**:79–85. http://dx.doi.org/10.1016/S0944-5013(00)80041-5.

28. **Payne AN, DiChristina TJ.** 2006. A rapid mutant screening technique for detection of technetium [Tc(VII)] reduction-deficient mutants of *Shewanella oneidensis* MR-1. FEMS Microbiol Lett **259**:282–287. http://dx.doi.org/10.1111/j.1574-6968.2006.00278.x.

29. **Miller GL.** 1959. Use of dinitrosalicylic acid reagent for determination of reducing sugar. Anal Chem **31**:426–428. http://dx.doi.org/10.1021/ac60147a030.

30. **Geer LY, Marchler-Bauer A, Geer RC, Han L, He J, He S, Liu C, Shi W, Bryant SH.** 2010. The NCBI Biosystems database. Nucleic Acids Res **38**:D492–D496. http://dx.doi.org/10.1093/nar/gkp858.

31. **Roy A, Kucukural A, Zhang Y.** 2010. I-TASSER: a unified platform for automated protein structure and function prediction. Nat Protoc **5**:725–738. http://dx.doi.org/10.1038/nprot.2010.5.

32. **Agrawal M, Chen RR.** 2011. Discovery and characterization of a xylose reductase from *Zymomonas mobilis* ZM4. Biotechnol Lett **33**:2127–2133. http://dx.doi.org/10.1007/s10529-011-0677-6.

33. **Akinterinwa O, Cirino PC.** 2009. Heterologous expression of D-xylulokinase from *Pichia stipitis* enables high levels of xylitol production by engineered *Escherichia coli* growing on xylose. Metab Eng **11**:48–55. http://dx.doi.org/10.1016/j.ymben.2008.07.006.

34. **McCorkindale J, Edson NL.** 1954. Polyol dehydrogenases. I. The specificity of rat-liver polyol dehydrogenase. Biochem J **57**:518–523.

35. **Burns JL, Ginn BR, Bates DJ, Dublin SN, Taylor JV, Apkarian RP, Amaro-Garcia S, Neal AL, DiChristina TJ.** 2010. Outer membrane-associated serine protease involved in adhesion of *Shewanella oneidensis* to Fe(III) oxides. Environ Sci Technol **44**:68–73. http://dx.doi.org/10.1021/es9018699.

36. **Sievers F, Wilm A, Dineen D, Gibson TJ, Karplus K, Li WZ, Lopez R, McWilliam H, Remmert M, Soding J, Thompson JD, Higgins DG.** 2011. Fast, scalable generation of high-quality protein multiple sequence alignments using Clustal Omega. Mol Syst Biol **7**:539. http://dx.doi.org/10.1038/msb.2011.75.

37. **Kratschmar D, Wallner S, Florenski S, Schmid D, Kuhn R.** 1999. Analysis of oligosaccharides by MEKC with aminobenzoic alkyl esters as derivatization agents. Chromatographia **50**:596–600. http://dx.doi.org/10.1007/BF02493666.

38. **Montgomery H, Dymock JF.** 1962. The rapid determination of nitrite in fresh and saline waters. Analyst **87**:374–378. http://dx.doi.org/10.1039/an9628700374.

39. **Metzger MH, Hollenberg CP.** 1995. Amino acid substitutions in the yeast *Pichia stipitis* xylitol dehydrogenase coenzyme-binding domain affect the coenzyme specificity. Eur J Biochem **228**:50–54. http://dx.doi.org/10.1111/j.1432-1033.1995.tb20227.x.

40. **Di Luccio E, Petschacher B, Voegtli J, Chou HT, Stahlberg H, Nidetzky B, Wilson DK.** 2007. Structural and kinetic studies of induced fit in xylulose kinase from *Escherichia coli*. J Mol Biol **365**:783–798. http://dx.doi.org/10.1016/j.jmb.2006.10.068.

41. **Kanehisa M, Goto S.** 2000. KEGG: Kyoto Encyclopedia of Genes and Genomes. Nucleic Acids Res **28**:27–30. http://dx.doi.org/10.1093/nar/28.1.27.

42. **Myers CR, Nealson KH.** 1988. Bacterial manganese reduction and growth with manganese oxide as the sole electron acceptor. Science **240**:1319–1321. http://dx.doi.org/10.1126/science.240.4857.1319.

43. **Cooper R, Goff J, Reed B, Sekar R, DiChristina TJ.** 2015. Breathing iron: molecular mechanism of microbial iron reduction by *Shewanella oneidensis*, p 5.2.1-1–5.2.1–13. *In* Yates M, Nakatsu C, Miller R, Pillai S (ed), Manual of environmental microbiology, 4th ed. ASM Press, Washington, DC.

44. **Jeon JM, Park H, Seo HM, Kim JH, Bhatia SK, Sathiyanarayanan G, Song HS, Park SH, Choi KY, Sang BI, Yang YH.** 2015. Isobutanol production from an engineered *Shewanella oneidensis* MR-1. Bioprocess Biosyst Eng **38**:2147–2154. http://dx.doi.org/10.1007/s00449-015-1454-z.

45. **Visser EM, Leal TF, de Almeida MN, Guimaraes VM.** 2015. Increased enzymatic hydrolysis of sugarcane bagasse from enzyme recycling. Biotechnol Biofuels **8**:5. http://dx.doi.org/10.1186/s13068-014-0185-8.

46. **Shinnick SG, Perez SA, Varela MF.** 2003. Altered substrate selection of the melibiose transporter (MelY) of *Enterobacter cloacae* involving point mutations in Leu-88, Leu-91, and Ala-182 that confer enhanced center dot maltose transport. J Bacteriol **185**:3672–3677. http://dx.doi.org/10.1128/JB.185.12.3672-3677.2003.

47. **King SC, Wilson TH.** 1990. Identification of valine 177 as a mutation altering specificity for transport of sugars by the *Escherichia coli* lactose carrier-enhanced specificity for sucrose and maltose. J Biol Chem **265**:9638–9644.

48. **Van Camp BM, Crow RR, Peng Y, Varela MF.** 2007. Amino acids that confer transport of raffinose and maltose sugars in the raffinose permease (RafB) of *Escherichia coli* as implicated by spontaneous mutations at Val-35, Ser-138, Ser-139, Gly-389 and Ile-391. J Membr Biol **220**:87–95. http://dx.doi.org/10.1007/s00232-007-9077-1.

49. **Sun L, Zeng X, Yan C, Sun X, Gong X, Rao Y, Yan N.** 2012. Crystal structure of a bacterial homologue of glucose transporters GLUT1–4. Nature **490**:361–366. http://dx.doi.org/10.1038/nature11524.

50. **Sekar R, DiChristina TJ.** 2014. Microbially driven Fenton reaction for degradation of the widespread environmental contaminant 1,4-dioxane. Environ Sci Technol **48**:12858–12867. http://dx.doi.org/10.1021/es503454a.

51. **Dehio C, Meyer M.** 1997. Maintenance of broad-host-range incompatibility group P and group Q plasmids and transposition of Tn*5* in *Bartonella henselae* following conjugal plasmid transfer from *Escherichia coli*. J Bacteriol **179**:538–540.

52. **Kovach ME, Phillips RW, Elzer PH, Roop RM, Peterson KM.** 1994. pBBR1MCS: a broad-host-range cloning vector. Biotechniques **16**:800–802.